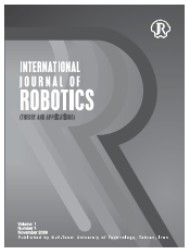

INTERNATIONAL JOURNAL OF ROBOTICS
(THEORY AND APPLICATIONS)
E-mail: IJR@kntu.ac.ir

Robust Trajectory Free Model Predictive Control of Biped Robots with Adaptive Gait Length

M. Parsa[a] and M. Farrokhi[a]

a- Department of Electrical Engineering, Iran University of Science and Technology, Tehran, 16846-13114, IRAN, E-mail: farrokhi@iust.ac.ir.

ARTICLE INFO

Keywords:
Biped Robots
Model Predictive Control
Disturbance Observer
Gait Length

ABSTRACT

This paper employs nonlinear disturbance observer (NDO) for robust trajectory-free Nonlinear Model Predictive Control (NMPC) of biped robots. The NDO is used to reject the additive disturbances caused by parameter uncertainties, unmodeled dynamics, joints friction, and external slow-varying forces acting on the biped robots. In contrary to the slow-varying disturbances, handling sudden pushing disturbances acting on the biped robots is much more complicated and using the NDO doesn't guarantee the biped walking stability. In order to reject these kinds of disturbances, the motion controller must be able to make suitable decisions for quick changing of the gait length or the walking speed. However, the gait length change is not possible while tracking fixed predefined joint trajectories. Hence, in this paper the NMPC is designed in such a way that it has the ability to change the gait length appropriately. In addition, some schemes will be proposed to reduce the computation time of the NMPC. Simulating results show good performance of the proposed method in trajectory-free walking of biped robots as well as disturbance rejection.

1. Introduction

Development of legged locomotion systems has recently received an increasing attention due to their higher mobility than conventional wheeled vehicles. Legs are adapted to cluttered environments allowing the machine to stride over obstacles and limiting the damages to the environment thanks to their small supporting surface. An important branch of the legged robots are the biped robots, which are based on the human oriented facilities. The biped robots are expected to imitate human behaviors and locomotion abilities, e.g. getting up and down the stairs and ladders and passing uneven and rough grounds. Some of these demands, which are not achievable by the wheeled robots, emphasize more on the use of the biped robots. These new demands together with the new concepts in the field of biped robots (i.e. providing stable walking and balance to the biped robot) demand applying new and well adapted motion control approaches. Practically, there may be some uncertainties in the biped robot parameters and/or parameter variations in the biped dynamics. Moreover, there are some unmodeled dynamics in the biped robot model. In addition, joints friction and external slow varying forces acting on the biped robots usually exist. Hence, an unavoidable property of the biped motion controller that has to be concerned with is its robustness. Recently, some robust biped motion control methods have been proposed by researchers. For instance, in [1] the controller is designed based on constructing an error vector between the robot measurable states and the desired states then forcing the gradient of this error vector to be negative via the use of a suitable Lyapunov function. The controller is robust in the sense that it accommodates unstructured uncertainties inherent in robotics. Reference [2] has suggested a robust controller with modeling uncertainties and external disturbances for stable dynamic walking of biped robots. In [3], the finite-time robust trajectory tracking control strategy is designed to make the states of the system reach the tracking target point in finite time. This control strategy is based on the theory of Lyapunov stability and the characteristics of the system. This control strategy can make the error be bounded in terminal value under the condition of external uncertain disturbances, otherwise be zero. Robust control methods, especially in the nonlinear systems, have usually complicated theories and need some knowledge about the uncertainty structure, such as the upper bound of disturbances. One of the indirect methods to robust a controller that has received more attention during the past

years, is the Disturbance Observer Based Control (DOBC). The Disturbance Observer (DO) is a robust compensator proposed by Ohnishi in 1987 [4]. The main idea behind developing a disturbance observer can be stated as: First, the DO estimates the equivalent disturbance and then the estimated disturbance is fed back as a cancellation signal and makes the whole system to behave like the nominal system. Since the DOBC scheme has simple structure and powerful performances, it is widely used for improving disturbance rejection performance and robustness in various mechanical servo systems [5-7]. One of the advantages of DOBC is that this method doesn't need upper norm band of the uncertainty. The other advantage is that it helps to robust control methods which are not robust by their own. Hence, DOBC can be used to construct a controller for the bipeds, which provide robustness to the controller. Based on this view, selecting the motion control method may be a challenging decision.

Noticing at the previously mentioned biped robust controllers, it's observed that a common property of these approaches is that they all try to reduce the tracking error of the trajectory produced by the gait planner block; whereas comparing by human walking nature, defining a trajectory and consuming more efforts to track it may not be suitable. The biped robot may have a normal and acceptable walk even if there are some errors in the trajectory tracking of the joints. On the other hand, a worthy trajectory has to consider the biped physical constraints together with actuators capability while minimizing the energy consumption. Based on these ideas, [8] has proposed a trajectory free motion control of bipeds based on the Nonlinear Model Predictive Control (NMPC). This paper has considered only the Single Support Phase (SSP) of the robot. In [9] the controller is improved and the Double Support Phase (DSP) has been also added. Also [10] has used the same method while it has claimed a real-time algorithm. It should be mentioned that all previous papers are model based methods, which have tried to use the advantage of omitting the trajectory generation phase in the biped motion control. In addition to low robust characteristics, a common problem in these papers is that the gait length is kept fixed. Letting the NMPC to change the gait length causes more flexibility and also improves the ability of the controller to maintain stability in presence of sudden disturbances.

The aim of this paper is to propose a robust biped motion control with less limitation as compared to the previously proposed methods. Thus a robust trajectory free nonlinear model predictive control based on disturbance observer is proposed in this paper. Moreover, the NMPC is designed in such a way that the gait length may be changed in presence of sudden disturbances to maintain the biped balance. In addition, some schemes will be proposed to reduce the computational time of the NMPC.

This paper is organized as follows. Section II presents dynamics of the 5-link planar biped robot in the SSP and DSP, and the impact effect. Section III provides the proposed NMPC strategy by defining an appropriate objective function and the constraints. In Section IV, the NDO is added to the control loop to insure the controller robustness. Section V shows simulation results. Section VI concludes this paper.

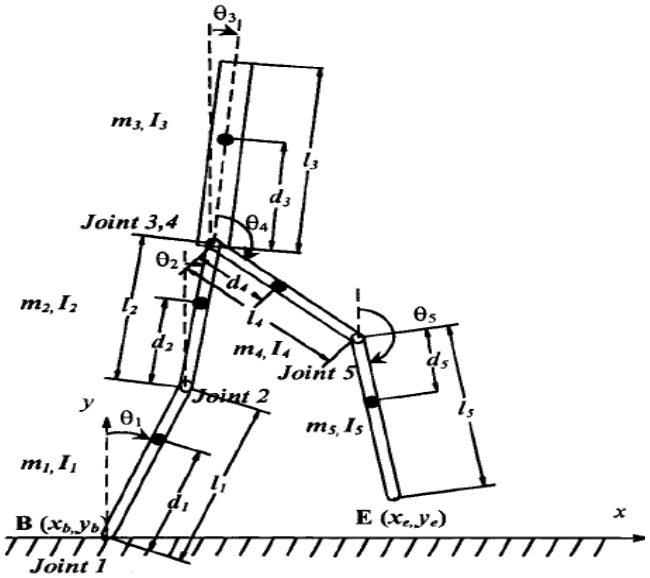

Fig. 1. Planar five link biped robot model [11].

2. Five-Link Biped Robot Dynamics

In this paper, the control of a planar biped robot with five links is considered. This biped contains a torso and two identical lower limbs with each limb having a thigh and a shank (Fig. 1). Moreover, the biped has two hip joints, two knee joints, and two ankles at tips of the lower limbs. There is an actuator located at each joint; all joints are considered rotating in the sagittal plane. In addition, in this model, feet have no mass. This assumption simplifies the biped model while does not reduce that much efficiency of the biped dynamics [11]. Although the dynamics of the feet are neglected, it is assumed that the biped can apply torque at the ankles. Each gait consists of two successive dynamic: 1) The single support phase (SSP), where a stance limb is in contact with ground and the other limb swings from rear to front, and 2) The double support phase (DSP), where both limbs are on the ground while the body can slightly move forward. The impact happens in an infinitesimal period of time as the swing limb collides with the ground and joint velocities are subjected to a sudden jump resulting from this impact event. During the DSP, a torque is applied at leading ankle whereas the rear ankle does not possess a torque but can rotate through the knee torque and the effect of gravity. The friction between the feet and the ground is assumed sufficient to prevent slippage during walking graphic [11].

A. Single Support Phase

The biped locomotion with single foot support can be considered as an open-loop kinematic chain model [12].

The dynamic equations to describe the biped SSP can be derived using the standard procedure of Lagrangian formulation as

$$\mathbf{D}(\boldsymbol{\theta})\ddot{\boldsymbol{\theta}} + \mathbf{H}(\boldsymbol{\theta},\dot{\boldsymbol{\theta}})\dot{\boldsymbol{\theta}} + \mathbf{G}(\boldsymbol{\theta}) = \mathbf{T} \quad (1)$$

where $\mathbf{D}(\boldsymbol{\theta})$ is a 5×5 positive definite and symmetric matrix of inertia, $\mathbf{H}(\boldsymbol{\theta})$ is a 5×5 matrix related to the centrifugal and Coriolis terms, $\mathbf{G}(\boldsymbol{\theta})$ is a 5×1 vector of gravity terms, $\boldsymbol{\theta}$, $\dot{\boldsymbol{\theta}}$, $\ddot{\boldsymbol{\theta}}$, and $\mathbf{T}$ are 5×1 vectors of generalized coordinates, velocities, acceleration and torques, respectively [11].

B. Double Support Phase

The DSP begins with the front limb touching the ground and ends with the rear limb taking off the ground. As both of the contact points between the lower limbs and the ground are fixed during the DSP, there exists a set of holonomic constraints as

$$\boldsymbol{\Phi}(\boldsymbol{\theta}) = \begin{pmatrix} x_e - x_b - L \\ y_e - y_b \end{pmatrix} = 0 \quad (2)$$

where L is the step length and x_{b} and x_{e} are the stance foot and the swing tip position, respectively. Hence, the Lagrangian equation of motion during the DSP is

$$\mathbf{D}(\boldsymbol{\theta})\ddot{\boldsymbol{\theta}} + \mathbf{H}(\boldsymbol{\theta},\dot{\boldsymbol{\theta}})\dot{\boldsymbol{\theta}} + \mathbf{G}(\boldsymbol{\theta}) = \mathbf{J}^{\mathrm{T}}(\boldsymbol{\theta})\boldsymbol{\lambda} + \mathbf{T} \quad (3)$$

where $\boldsymbol{\lambda}$ is the vector of Lagrange multipliers and $\mathbf{J} = \partial\boldsymbol{\Phi}/\partial\boldsymbol{\theta}$ is the 2×5 Jacobian matrix. As a dynamic system under holonomic constraint, a set of independent generalized coordinate can be found to formulate the dynamic equations, which describe the constraint system without using the terms of constraint forces [13]. Let the independent generalized coordinate be $\mathbf{p} = \begin{pmatrix} x_h & y_h & \theta_3 \end{pmatrix}^{\mathrm{T}}$, where $\begin{pmatrix} x_h & y_h \end{pmatrix}$ is the hip position. With this new coordinates, (3) can be written as

$$\ddot{\mathbf{p}}(\boldsymbol{\theta}) = \mathbf{B}\mathbf{p}(\boldsymbol{\theta}) + \mathbf{C}\left(\mathbf{T} - \mathbf{N}\right) \quad (4)$$

where $\mathbf{B}$ is a 3×3 matrix, $\mathbf{C}$ is a 3×5 matrix and $\mathbf{N}$ is a 5×1 vector [11].

C. Impact Effect

At the end of the SSP, the tip of the swing limb contacts the ground surface with an impact. The joint velocities are subjected to a sudden jump resulting from this impact event. The vertical velocity of the tip of the swing limb becomes zero immediately after the impact due to the ground collision

$$\dot{\boldsymbol{\theta}}^{+}_{\mathrm{impact}} = \dot{\boldsymbol{\theta}}^{-} + \mathbf{D}^{-1}\mathbf{J}^{\mathbf{T}}\left[\mathbf{J}\mathbf{D}^{-1}\mathbf{J}^{\mathbf{T}}\right]^{-1}\left(-\mathbf{J}\dot{\boldsymbol{\theta}}^{-}\right) \quad (5)$$

where $\dot{\boldsymbol{\theta}}^{+}_{\mathrm{impact}}$ and $\dot{\boldsymbol{\theta}}^{-}$ are 5×1 vectors of generalized velocities immediately after and before the impact, respectively [11].

3. NMPC Control Approach

The ordinary motion control methods in robotics are comprised of two phases: 1) the motion planning phase [14] and 2) the trajectory following phase. In the biped robots, the motion planning (i.e. the gait generation) phase may be performed off-line or on-line [9]. The offline gait generation cannot adapt to the environment changes like obstacles, which can reduce the robot's abilities to walk. There are different methods for the on-line gait generation that can adapt to the environment. An on-line adaptive optimal gait pattern would facilitate best the biped robot motion control. Although consuming more efforts to reduce the error of tracking is the goal of lots of control problems, perfect joint trajectory tracking is not necessary in the biped motion control since the biped robot may have normal and acceptable walk even if there are some errors in the trajectory tracking of the joints. Thus, ordinary robot motion planning methods may not fit well to the biped robots. The Human walking approach is based on optimal algorithms, which use some goals and constraints to displace the body or the Center of Mass (CoM) from one point to another, while considering and predicting the environment changes, in order to decide adaptively to accomplish safe and without falling walk [9]. A suitable way of imitating this behavior for motion control of the biped robot is to state the problem as a non-linear model based predictive control [15-17]. With an appropriate objective function, while considering the state and the control signal constraints plus the physical constraints, it is possible to combine the gait pattern generation phase with the control phase and allowing the NMPC to decide about both the gait pattern and the control signals. In this approach, there are no trajectories to follow. Instead, the control signals are generated by the NMPC directly in such a way that the biped robot is able to walk. In addition to the advantages of the on-line gait generation, this method considers the biped dynamics, constraints of the control signals, the present and the future of the biped states, and the physical constraints in the robot to execute more optimal and practical walking.

As declared in the literature review, some papers have focused on the trajectory free NMPC control [8-10]; but a common problem in these papers is that the gait length is kept fixed or there is not an appropriate approach to change it. In a complete walking cycle, the biped has to start walking when it is in a stand up position. After some steps it must reach a stable limit cycle, which means almost a constant body progression speed and constant gait length. Then, reaching the destination, the walking progression speed and constant gait length has to reduce and finally the biped has to stop covering the desired displacement. On the other hand, the gait length can affect the energy consumption and walking stability. In addition, gait length plays an important role in handling of external sudden disturbance. Thus, letting the NMPC to adjust the length might be a good idea, which is achieved in this paper by redefining some constraints. Solving the whole

problem using three NMPC instead of one, is another contribution of this paper. In previous papers, there is one NMPC that is responsible for the biped motion control. Due to the nonlinearity of the optimization problem, the NMPC that solves a large problem is divided into three NMPC each of which concentrates to limited constraints with an appropriate objective function. In this way, the computation time can be reduced substantially. It seems that the stance foot containing link one and two, the swing foot containing link four and five, and link three, which is the torso, have different responsibilities and constraints during walking. Thus there may be three NMPCs each controlling one of the mentioned parts. These NMPCs work in series with each other. This procedure is followed in the subsections.

A. Single Support Phase

The stance foot plays an important role in the body progression during SSP and DSP. Thus, starting with the stance foot controller sounds a logical choice. Adjusting walking speed is the other responsibility of the stance foot. This NMPC has to cover constraints such as feasible angles for joints one and two, guarantying static stability, constraints for moving forward, and the hip height. These demands are considered as the objective function and constraints given as

$$J_{\text{Stance}} = w_1^{St} \sum_{i=0}^{N_C^{St}-1} \mathbf{T}_{1,2}\left(t+i\Delta t\right)^T \mathbf{T}_{1,2}\left(t+i\Delta t\right) + w_2^{St} \sum_{j=1}^{N_P^{St}} \left(\dot{x}_{CoM}\left(t+j\Delta t\right) - \alpha \dot{x}_{CoM}^d\right)^2 \quad (6)$$

subject to

1) Constraints for the angle of joints one and two

$$q_{i,\min} \le q_i \le q_{i,\max} \quad (i=1,2),\ q_1 = \frac{\pi}{2} - \theta_1,\quad q_2 = \pi + \theta_1 - \theta_2 \quad (7)$$

2) The moving forward constraint

$$\dot{x}_{CoM} \ge 0 \quad (8)$$

3) The upper and lower bound of the hip height

$$h_{\min} \le h_{hip} \le h_{\max} \quad (9)$$

4) The upper and lower bound of the control torque

$$T_{i,\min} \le T_i \le T_{i,\max} \quad i=1,2 \quad (10)$$

5) And the static stability constraint

$$\begin{aligned} x_{\min}^{\text{DSP}}\left(k\right) \le x_{CoM} \le x_{\max}^{\text{DSP}}\left(k\right) \quad \text{for DSP} \\ x_{\min}^{\text{SSP}}\left(k\right) \le x_{CoM} \le x_{\max}^{\text{SSP}}\left(k\right) \quad \text{for SSP} \end{aligned} \quad (11)$$

where $N_C^{St}, N_P^{St}, w_1^{St}$ and w_2^{St} are the control and prediction horizons, energy consumption of link one and two and the progression speed weights, respectively. The horizontal speed centre of mass (CoM) has been selected as candidate of the biped walking speed. The NMPC optimizer tries to follow the desired $\alpha \dot{x}_{CoM}^d$ while α adjust the desired speed. Approaching the destination, the desired speed reduces exponentially as

$$\alpha = 1 - 2/\left(1+\exp\left(\frac{x_{CoM}^d - \hat{x}_{CoM}\left(t+j\Delta t\right)}{\sigma}\right)\right) \quad (12)$$

where x_{CoM}^d is the desired displacement of the CoM and σ is a designing parameter, $x_{\min}^{\text{DSP}}\left(k\right)$, $x_{\max}^{\text{DSP}}\left(k\right)$, $x_{\min}^{\text{SSP}}\left(k\right)$, and $x_{\max}^{\text{SSP}}\left(k\right)$ are shown in Fig. 2.

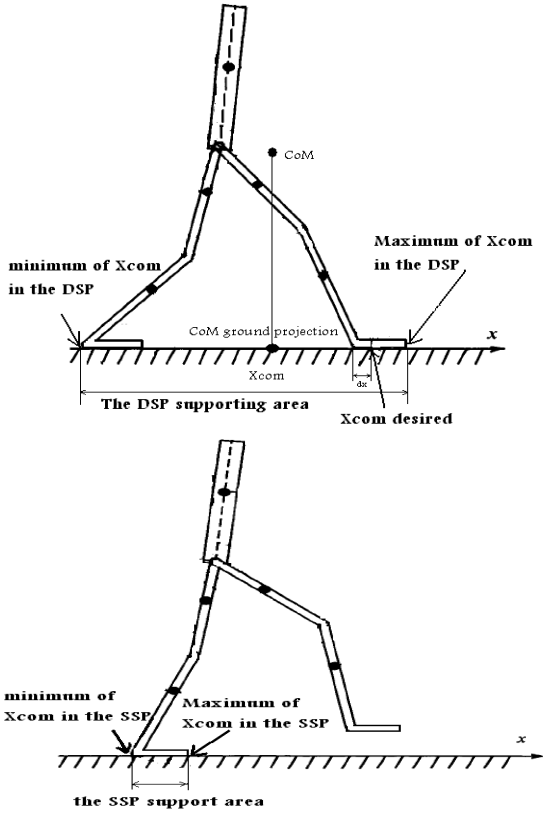

Fig. 2. DSP and SSP supporting area and their margins.

B. Swing Foot Control

Using the optimized torques of joint one and two, the second NMPC starts its operation to generate appropriate torques for joint four and five. These torques must force the swing foot to move in a parabolic path in the sagittal plane. The second NMPC achieves this goal by complying the horizontal and vertical speed constraints of the swing foot and some other constraints. In addition to the energy consumption cost of joints four and five, there is another term that forces the swing foot to reduce its height while CoM reaches its higher margin. This term may change the step length and force the swing foot to land quickly when CoM reaches to its higher margin sooner than usual. This situation may be caused by a sudden pushing disturbance. Thus, this term may help the biped to recover its balance. Therefore, the second NMPC objective function and its constraints can be stated as

$$J_{\text{Swing}}^{SSP} = w_1^{Sw} \sum_{i=0}^{N_c^{Sw}-1} \mathbf{T}_{4,5}\left(t+i\Delta t\right)^T \mathbf{T}_{4,5}\left(t+i\Delta t\right) + \sum_{j=1}^{N_p^{Sw}} w_2^{Sw}(j)\,\hat{y}_e\left(t+j\Delta t\right) \quad (13)$$

subjected to

1) Constraints for the angle of joints four and five

$$q_{i,\min} \le q_i \le q_{i,\max} \; (i=4,5), \;\; q_4 = \theta_4, \;\; q_5 = \pi + \theta_5 - \left(\theta_3 + \theta_4\right) \quad (14)$$

2) The lower and upper bound of the control torque constraints

$$T_{i,\min} \le T_i \le T_{i,\max} \quad i = 4,5 \quad (15)$$

3) The lower and upper bound of the swing foot height constraints

$$y_b \le y_e \le y_b + h_{\text{m}} \quad (16)$$

4) The horizontal speed of the swing foot constraints

$$\beta_{\min}\dot{x}_{CoM} \sin\left(\frac{y_e - y_b}{h_{\max}}\frac{\pi}{2}\right) \le \dot{x}_e \le \beta_{\max}\dot{x}_{CoM} \sin\left(\frac{y_e - y_b}{h_{\max}}\frac{\pi}{2}\right) \quad (17)$$

5) The vertical speed of the swing foot constrain

$$\delta\dot{x}_{CoM} \sin\left(\frac{|x_e - x_b|}{L}\pi\right) \sin\left(\frac{y_e - y_b}{h_{\max}}\pi\right) + sgn\left(x_e - x_b\right)\dot{y}_e \le 0 \quad (18)$$

where N_C^{Sw}, N_P^{Sw}, w_1^{Sw} and w_2^{Sw} are the control and the prediction horizons, the energy consumption cost of links four and five, and the penalty for the swing foot height, respectively, $\left(x_b, y_b\right)^T$ and $\left(x_e, y_e\right)^T$ are the base and the swing foot tip positions, respectively, L is the length of the previous gait, and h_m is the maximum allowable height of the swing foot. Eqs. (17) and (18) adjust the horizontal and vertical speed of the swing foot while synchronizing them with the CoM horizontal speed. It should be noted that no desired gait length is considered in these equations; hence, it's free to change. Eq. (17) forces the horizontal position of the swing foot to be zero when it lands. Eq. (18) adjusts the vertical speed of the swing foot vertical based on its horizontal and vertical positions. $\beta_{\min}$, $\beta_{\max}$, and δ are tuning parameters and w_2^{Sw} is

$$w_2^{Sw}(j) = \begin{cases} 0 & \hat{x}_e(t+j\Delta t) \le x_b \\ \eta\, e^{\left(\frac{FL+\varepsilon}{FL+x_b+\varepsilon-x_{CoM}(j)}-1\right)} & \hat{x}_e(t+j\Delta t) > x_b \end{cases} \quad (19)$$

where FL is the foot length. As soon as the CoM reaches its maximum allowable position, which is equal to $FL + x_b$, w_2^{Sw} grows exponentially and increases the cost of the swing foot height. ε is a designing constant to prevent w_2^{Sw} to become infinite. It must be noted that during the DSP the swing foot has to remain on the ground and thus, the NMPC for DSP reduces to

$$J_{\text{Swnig}}^{\text{DSP}} = \sum_{i=0}^{N_c^{Sw}-1} \mathbf{T}_{4,5}\left(t+i\Delta t\right)^T \mathbf{T}_{4,5}\left(t+i\Delta t\right) \quad (20)$$

Subject to (14) while satisfying $y_e = y_b$.

C. Torso Angle Control

Using the optimized torques of joints one, two, four and five, the third NMPC generates appropriate torque for joint three. The torso contains a major part of the biped weight. Thus, it may strongly affect the CoM and the biped stability. The third NMPC has to limit the torso angle in an acceptable region while satisfying the static stability. The third NMPC is given as

$$J_{\text{Torso}} = \sum_{i=0}^{N_c^{To}-1} \left[T_3\left(t+i\Delta t\right)\right]^2 \quad (21)$$

subjected to

1) The torso allowable angle

$$\alpha_{\min} \le \theta_3 \le \alpha_{\max} \quad (22)$$

2) The lower and upper bound of the control torque constraint

$$T_{3,\min} \le T_3 \le T_{3,\max} \quad (23)$$

3) The biped static stability constraint

$$\begin{aligned} x_{\min}^{\text{DSP}}(k) \le x_{CoM} \le x_{\max}^{\text{DSP}}(k) \quad &\text{for DSP} \\ x_{\min}^{\text{SSP}}(k) \le x_{CoM} \le x_{\max}^{\text{SSP}}(k) \quad &\text{for SSP} \end{aligned} \quad (24)$$

where N_C^{To} is the control horizon, and $\alpha_{\min}$ and $\alpha_{\max}$ are the minimum and maximum torso angles.

4. NONLINEAR DISTURBANCE OBSERVER

As stated in introduction, the aim of this paper is to propose a robust biped motion control with fewer limitations as compared to the methods proposed in literatures, while it rejects external disturbances appropriately. To this end, Disturbance Observer (DO) based control (an indirect robust control) method is adopted in this paper. In the previous section, the trajectory free NMPC was designed as the main controller. In this section, an appropriate DO is designed and added to the control loop. Although different DOs exist in literature, they can be classified into two categories: Linear DO (LDO) and Nonlinear DO (NDO). Although LDO have been applied to many nonlinear systems, but it may reduce the robustness of the closed-loop system, especially for highly nonlinear systems like bipeds. Therefore, in this paper an NDO is designed and employed. This DO contains nonlinear dynamics of the system and its stability can be guaranteed by Lyapunov methods. In [18] a Lyapunov-based NDO for a serial *n*-link manipulators has been proposed. Using the similarity between the SSP of the biped dynamic and the manipulator dynamic, the proposed NDO may be a good selection. However, the DSP dynamic of biped is slightly different from the manipulator dynamic. As soon as the swing foot of the biped touches the ground, a 2×1 vector of external forces (caused by the horizontal and vertical ground reactions and frictions) is added to the biped input. Treating the DSP dynamics as the SSP dynamics, the NDO detects these external forces as disturbances and

tries to omit them. Zero reaction forces means the biped has started the SSP, which contradicts with the real dynamic of the biped. The biped inertial matrix differs from the manipulator inertial matrix used in the [18]; thus, some modification in the NDO design is needed. In the followings the NDO is designed and added to the control loop.

Using (3) and assuming additive disturbances, the overall biped dynamic becomes

$$\mathbf{D_n}(\boldsymbol{\theta})\ddot{\boldsymbol{\theta}}+\mathbf{H_n}(\boldsymbol{\theta},\dot{\boldsymbol{\theta}})\dot{\boldsymbol{\theta}}+\mathbf{G_n}(\boldsymbol{\theta})=\mathbf{T_n}+\mathbf{T_{dist}}+\mathbf{J}^T\boldsymbol{\lambda}_\mathbf{n} \quad (25)$$

where $\mathbf{D_n}$, $\mathbf{H_n}$ and $\mathbf{G_n}$ are the nominal inertial matrix, the nominal centrifugal and Coriolis terms, and the nominal gravity terms of the biped robot, respectively, $\mathbf{J^T}\boldsymbol{\lambda}_\mathbf{n}$ is the ground reaction vector while the biped parameters have nominal values. By defining $\mathbf{T_n'}=\mathbf{T_n}+\mathbf{J}^T\boldsymbol{\lambda}_\mathbf{n}$, (25) will be similar to the SSP dynamic. The additive disturbance may be divided to the internal and external disturbances as

$$\mathbf{T_{dist}}=\mathbf{T_{dist,ext}}+\mathbf{T_{dist,int}} \quad (26)$$

where $\mathbf{T_{dist,int}}=-\delta\mathbf{D}\ddot{\boldsymbol{\theta}}-\delta\mathbf{H}\dot{\boldsymbol{\theta}}-\delta\mathbf{G}$ is the additive uncertainty of the biped dynamics and $\mathbf{T_{dist,ext}}$ is the external disturbance vector that contains torques due to the unknown loads, external forces, friction forces, and torque ripples. According to [18], the disturbance observer dynamic may be designed as

$$\dot{\mathbf{e}}+\mathbf{L}(\boldsymbol{\theta},\dot{\boldsymbol{\theta}})\mathbf{e}=\mathbf{0} \quad (27)$$

where $\mathbf{e}=\mathbf{T_{dist}}-\hat{\mathbf{T}}_\mathbf{dist}$, in which $\hat{\mathbf{T}}_\mathbf{dist}$ is the observed disturbance. Assuming slow varying disturbances, $\dot{\mathbf{T}}_\mathbf{dist}$ can be omitted from (27). By appropriate design of $\mathbf{L}(\boldsymbol{\theta},\dot{\boldsymbol{\theta}})$, the NDO error may reduce exponentially and the disturbance would be observed. Substituting (25) in (27), the NDO dynamic is

$$\dot{\hat{\mathbf{T}}}_\mathbf{dist}=\mathbf{L}(\boldsymbol{\theta},\dot{\boldsymbol{\theta}})\begin{pmatrix}\mathbf{D_n}(\boldsymbol{\theta})\ddot{\boldsymbol{\theta}}+\mathbf{H_n}(\boldsymbol{\theta},\dot{\boldsymbol{\theta}})\dot{\boldsymbol{\theta}}+\\ +\mathbf{G_n}(\boldsymbol{\theta})-\mathbf{T_n'}-\hat{\mathbf{T}}_\mathbf{dist}\end{pmatrix}. \quad (28)$$

As (28) shows, the acceleration signal $\ddot{\boldsymbol{\theta}}$ is required to realize the DO. Since measuring acceleration is a difficult task in many robotic applications, the problem can be solved by defining an auxiliary variable $\boldsymbol{\Psi}=\hat{\mathbf{T}}_\mathbf{dist}-\mathbf{P}(\dot{\boldsymbol{\theta}})$ where $\mathbf{P}(\dot{\boldsymbol{\theta}})$ is defined as $\mathbf{P}(\dot{\boldsymbol{\theta}})=c\begin{bmatrix}\dot{\theta}_1 & \dot{\theta}_2 & \cdots & \dot{\theta}_5\end{bmatrix}^T$ and c is the observer gain[1]. Differentiating $\boldsymbol{\Psi}$ w.r.t. time and substituting into (28) gives

$$\dot{\hat{\mathbf{T}}}_\mathbf{dist}=\dot{\boldsymbol{\Psi}}+\frac{\partial\mathbf{P}(\dot{\boldsymbol{\theta}})}{\partial\dot{\boldsymbol{\theta}}}\ddot{\boldsymbol{\theta}} \quad (29)$$

$$\dot{\boldsymbol{\Psi}}+\frac{\partial\mathbf{P}(\dot{\boldsymbol{\theta}})}{\partial\dot{\boldsymbol{\theta}}}\ddot{\boldsymbol{\theta}}=\mathbf{L}(\boldsymbol{\theta},\dot{\boldsymbol{\theta}})\begin{pmatrix}\mathbf{D_n}(\boldsymbol{\theta})\ddot{\boldsymbol{\theta}}+\mathbf{H_n}(\boldsymbol{\theta},\dot{\boldsymbol{\theta}})\dot{\boldsymbol{\theta}}\\ +\mathbf{G_n}(\boldsymbol{\theta})-\mathbf{T_n'}-\hat{\mathbf{T}}_\mathbf{dist}\end{pmatrix} \quad (30)$$

Defining $\mathbf{L}(\boldsymbol{\theta},\dot{\boldsymbol{\theta}})=c\,\mathbf{D_n^{-1}}(\boldsymbol{\theta})$, the acceleration signal in (30) may be omitted and the simplified equation becomes

$$\dot{\boldsymbol{\Psi}}=\mathbf{L}(\boldsymbol{\theta},\dot{\boldsymbol{\theta}})\begin{pmatrix}\mathbf{H_n}(\boldsymbol{\theta},\dot{\boldsymbol{\theta}})\dot{\boldsymbol{\theta}}+\\ +\mathbf{G_n}(\boldsymbol{\theta})-\mathbf{T_n'}-\mathbf{P}(\dot{\boldsymbol{\theta}})-\boldsymbol{\Psi}\end{pmatrix}. \quad (31)$$

Based on Fig. 3, Eq. (31) may be rewritten as:

$$\dot{\boldsymbol{\Psi}}=\mathbf{L}(\boldsymbol{\theta},\dot{\boldsymbol{\theta}})\begin{pmatrix}\mathbf{H_n}(\boldsymbol{\theta},\dot{\boldsymbol{\theta}})\dot{\boldsymbol{\theta}}+\\ +\mathbf{G_n}(\boldsymbol{\theta})-\mathbf{T_c}-\mathbf{J}^T\boldsymbol{\lambda}_\mathbf{n}\end{pmatrix} \quad (32)$$

Based on the appendix in [11], $\boldsymbol{\lambda}_\mathbf{n}$ is

$$\boldsymbol{\lambda}_\mathbf{n}=-\mathbf{S_{c2,n}}^{-1}\left(\mathbf{S_{a21,n}}\dot{\boldsymbol{\omega}}+\mathbf{S_{b2,n}}\left(\mathbf{T_n}+\mathbf{T_{dist}}-\mathbf{N_n}\right)\right) \quad (33)$$

where $\mathbf{S_{c2,n}}$, $\mathbf{S_{a21,n}}$, $\dot{\boldsymbol{\omega}}$, $\mathbf{S_{b2,n}}$, and $\mathbf{N_n}$ are given in the appendix of [11]. According to the definition of the observation error in (33), $\boldsymbol{\lambda}_\mathbf{n}$ can be written as

$$\boldsymbol{\lambda}_\mathbf{n}=-\mathbf{S}_{\mathbf{c2,n}}^{-1}\left(\mathbf{S_{a21,n}}\dot{\boldsymbol{\omega}}+\mathbf{S_{b2,n}}\left(\mathbf{T_c}+\mathbf{e}-\mathbf{N_n}\right)\right) \quad (34)$$

where all terms are known. In must be noted that the NDO design in the SSP is the same as the DSP when $\boldsymbol{\lambda}_\mathbf{n}=0$.

In order to guarantee stability of the NDO, [18] has proposed a Lyapunov-based theorem to obtain the nonlinear disturbance observer gain c. This theorem is based on two properties:

Property I: $\mathbf{D_n}(\boldsymbol{\theta})$ is symmetric, positive definite, and bounded below and above, i.e., $\exists\,\alpha\geq\beta>0$ such that $\beta\mathbf{I}_n\leq\mathbf{D_n}(\boldsymbol{\theta})\leq\alpha\mathbf{I}_n, \forall\boldsymbol{\theta}\in\mathbf{R}^n$ where $\mathbf{I}_n$ is an $n\times n$ identity matrix.

Property II: The torque vector $\mathbf{T_n}$ is bounded. Thus, the angular velocity vector $\dot{\boldsymbol{\theta}}$ lies in a known bounded set. I.e., $\dot{\boldsymbol{\theta}}\in\boldsymbol{\Omega}_{\dot{\boldsymbol{\theta}}}\subset\left\{\dot{\boldsymbol{\theta}}:\left\|\dot{\boldsymbol{\theta}}\right\|\leq\dot{\boldsymbol{\theta}}_{\mathbf{max}}\right\}$.

As stated in Section II, $\mathbf{D_n}$ a positive definite and symmetric matrix. Thus, Property I is satisfied. Property II is properly true due to the constraints on the torque bound of the NMPCs. Based on the slight modification on $\mathbf{P}(\dot{\boldsymbol{\theta}})$ and following stability proof in [18], the allowed bound of NDO gain can be stated as

[1] In this paper $\mathbf{P}(\dot{\boldsymbol{\theta}})$ and $\mathbf{L}(\boldsymbol{\theta},\dot{\boldsymbol{\theta}})$ definition are slightly different from [18].

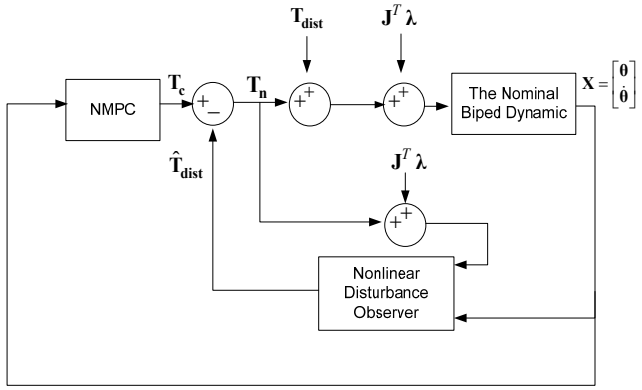

Fig. 3. Block diagram of the control method including NDO

$$c > \frac{n(n-1)}{4} \times \max\left\{\left|p_{21}\dot{\theta}_{21}\right|, \left|p_{31}\dot{\theta}_{31}\right|, \cdots, \left|p_{54}\dot{\theta}_{54}\right|\right\} \quad (35)$$
$$= 5 \times \max\left\{\left|p_{21}\dot{\theta}_{21}\right|, \left|p_{31}\dot{\theta}_{31}\right|, \cdots, \left|p_{54}\dot{\theta}_{54}\right|\right\}$$

where p_{ij} are constant parameters that depend on the masses and the length of the biped links, and *n* is the number of links.

The block diagram of the closed-loop system is shown in Fig. 3.

5. Simulation Results

Simulations are based on the biped BIP2000, which have been developed by Azevedo et al. [8, 9]. The physical parameters of this biped are given in Table I. In Table II, the maximum and minimum of the NMPC constraints have been listed. Moreover, the following values are used in the NMPC simulations:

$$N_C^{St} = N_C^{Sw} = N_C^{To} = 3 \qquad N_P^{St} = N_P^{Sw} = N_P^{To} = 3$$
$$\Delta t = 0.02\text{s} \quad FL = 0.2\text{m} \quad \sigma = 0.02,$$
$$\dot{x}_{CoM}^{d} = 0.3\,\text{m.s}^{-1} = 1.08\ \text{Km h}^{-1}$$
$$\beta_{\min} = 4 \quad \beta_{\max} = 6 \quad \delta = 1.5$$

According to (35), the observer would be globally asymptotically stable if parameter *c* is larger than 690. For faster convergence, this parameter has been selected equal to 1000 in simulations. The optimization problem is solved using the *fmincon* function in the MATLAB optimization toolbox dedicated to the minimization of a constrained nonlinear multivariable function. The *fmincon* is based on the sequential quadratic programming (SQP) algorithm. The SQP is an iterative technique in which the objective is replaced by a quadratic approximation and the constraints by linear approximations. Simulations are performed using Intel T7500 Core2 Duo 2.2 MHz processor with 1Gbyte of RAM.

The biped is supposed to start walking from the initial stand up orientation and follow a desired progression speed. As the biped reaches the destination, it has to reduce its speed and come to a complete stop passing 120 cm distance. All initial velocities and accelerations are set to zero. Knowing the position of the base foot, the biped orientation may be specified by the hip and swing foot positions. The initial orientation of the biped is selected near the stand up orientation as

$$x_e = -0.1\ \text{m}, \quad y_e = 0\ \text{m}, \quad x_h = -0.05\ \text{m}, \quad y_h = 0.7\ \text{m},$$

Simulations are carried out for three different cases. In the first case, the biped is exposed to slow varying disturbances. Internal disturbances are applied to the biped robot by 50% increase to the mass and inertia and 50% displacement of the centre of mass of all five links of the robot. Coulomb and viscous frictions and a constant torque of 30 Nm are exerted to all joints as the external disturbance. The Coulomb and viscous frictions is modeled as

$$T_{ext,i}^{dist} = K_{i1}\,\text{sign}\left(\dot{\theta}_i\right) + K_{i2}\dot{\theta}_i$$
$$K_{i1} = 50\ \text{Nm},\ K_{i2} = 6\ \text{Nm s rad}^{-1} \quad i = 1, \ldots, 5$$

In the second case, a sudden pushing disturbance at $t = 2$ s is exerted on the biped. This disturbance is modeled as an impact that has caused 5 deg and 1 rad/s sudden increase in the angular position and the velocity of the joint three, respectively.

In the third case, the effect of the measurement noise on the performance of the proposed method is examined. Gaussian noise with zero mean and variance equal to 0.01 and 0.1 are added to the angular position and velocity of joint three, respectively.

Simulation results are shown in Figs. 4 to 11. As Fig. 4 shows, the biped has started walking with zero initial velocity and has stopped by reducing its speed exponentially while it has passed 120 cm distance. The desired progression velocity is achieved. Although there are sudden decreases in the CoM velocity in the first steps while the biped switches from SSP to DSP, this problem is fading out in next steps. Fig. 5 shows that the swing foot has almost parabolic trajectory and the hip height changes are limited. In other words, the biped has smooth and normal walking. Figs. 6 and 7 show the exerted torque by the actuators and the estimated disturbance torque by the NDO, respectively. These figures exhibit that the NDO-based NMPC is able to handle slow varying disturbances caused by additive uncertainties and additive external torques. Fig. 8 shows that the horizontal position of the swing foot is clipped after the external sudden disturbance is exerted on the biped. This means that the gait length is shortened by the controller and the DSP has happened sooner in order to recover the static stability through establishing a wider supporting area. In order to evaluate the performance of the proposed method against measurement noise, a 10% Gaussian noise is added to the joint three, which has a profound role in the biped stability. Fig. 9 shows the angular velocity of joint three before and after of the measurement noise. Fig. 10

exhibits that the controller is able to attenuate the measurement noise. However, Fig. 11 shows that in order to overcome the measurement noise, higher frequencies appear in the control signals, may or may not be achievable in practice. Finally, Fig. 12 shows the performance of the NMPC for the case 1 but without NDO. As this figure shows, the biped is not able to maintain its stability and eventually falls down.

6. Conclusions

In this paper, the nonlinear disturbance observer was employed to robustify nonlinear model predictive control of biped robots. Defining a suitable objective function and appropriate constraints, the gait generation phase was discarded and included in the control phase using the NMPC. In contrast to the previous papers, which have defined fixed step length, in this paper, the step length can be changed by NMPC to optimize the energy consumption and stability. Using this ability, the controller may overcome sudden pushing disturbances by changing the gait length. The NDO improved robustness of the motion controller in the presence of the biped robot parameter variations and the unmodeled dynamics. Simulation results show that the proposed method has the ability to reject sudden pushing and slow varying disturbances. Handling sudden disturbances in the biped is much more complicated than stated in this paper and needs more attentions. Thus, improvement of push recovery ability of the controller may be a future work of this paper. Instead of using one NMPC confronting the whole problem, three smaller NMPCs were designed which work in series, consuming less computation time. Using this idea and trying to solving these three NMPCs in parallel may reduce the computation time more effectively.

TABLE 1: Physical parameters of robot [19]

Link No.	l_i Length (m)	m_i Mass (Kg)	I_i Inertia(Kg m^2)	d_i CoM (m)
1	0.41	5.93	0.69	0.258
2	0.41	10.9	1.31	0.258
3	0.5	48	18.99	0.391
4	0.41	10.9	1.31	0.258
5	0.41	5.93	0.69	0.258

TABLE 2: Maximum and minimum of constraints

Variable	l_i Length (m)	I_i Inertia (Kgm^2)
q_1	30°	120°
q_2, q_5	190°	270°
q_3, q_4	100°	240°
h_{hip}	0.68 m	0.72 m
θ_3	-3°	3°
h_m	0	0.05 m
T_i	-300 N.m	300 N.m

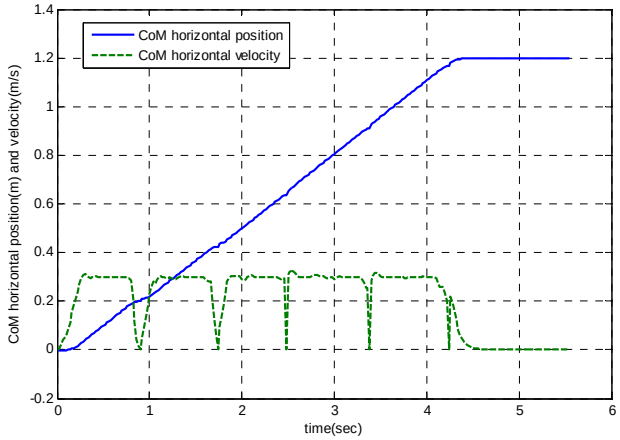

Fig. 4. Horizontal position and velocity of CoM with slow varying disturbances.

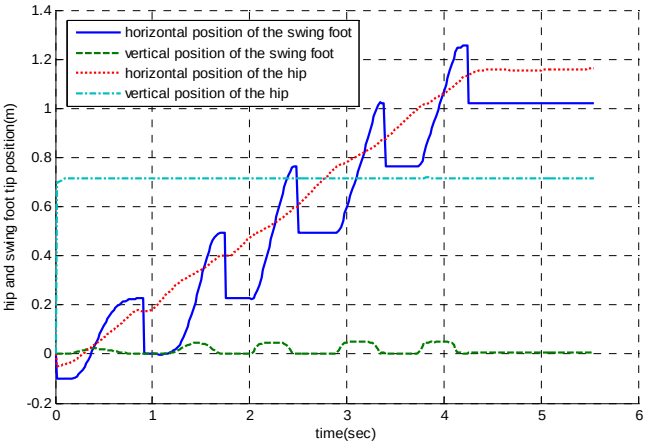

Fig. 5. Hip and swing foot tip vertical and horizontal positions with slow varying disturbances.

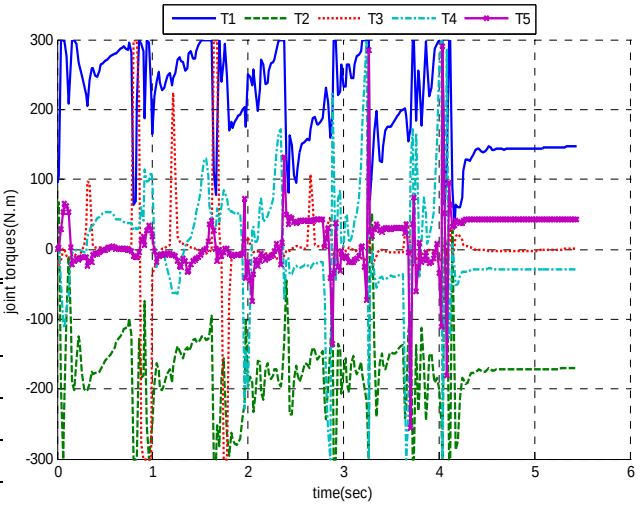

Fig. 6. Joint torques.

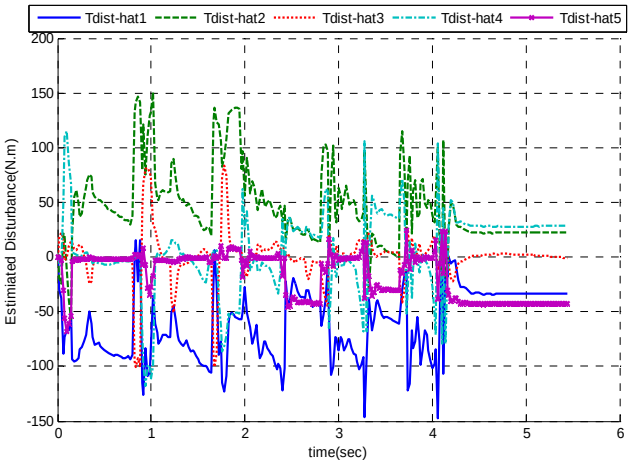

Fig. 7. Estimated disturbance torques.

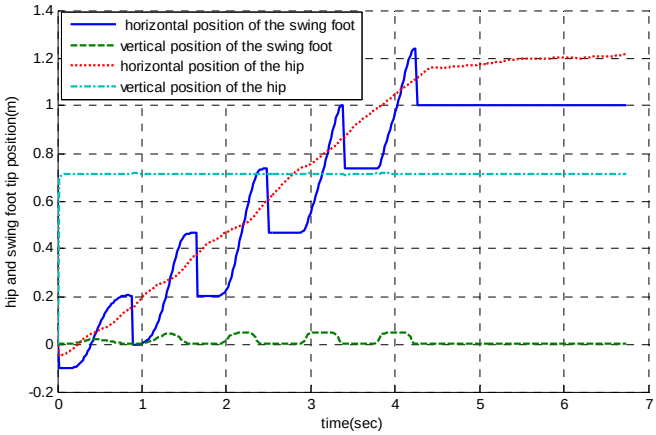

Fig. 10. Horizontal position and velocity of CoM with measurement noise

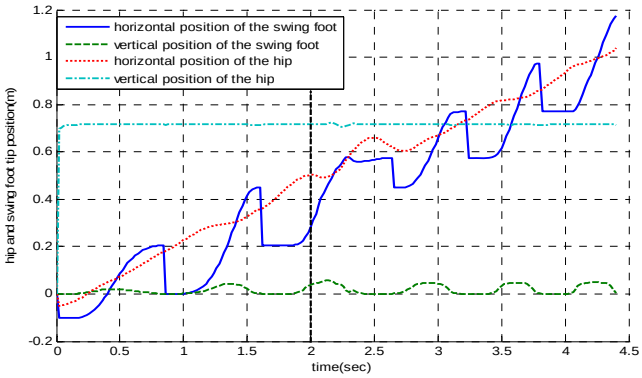

Fig. 8. Horizontal position and velocity of CoM with sudden pushing disturbances.

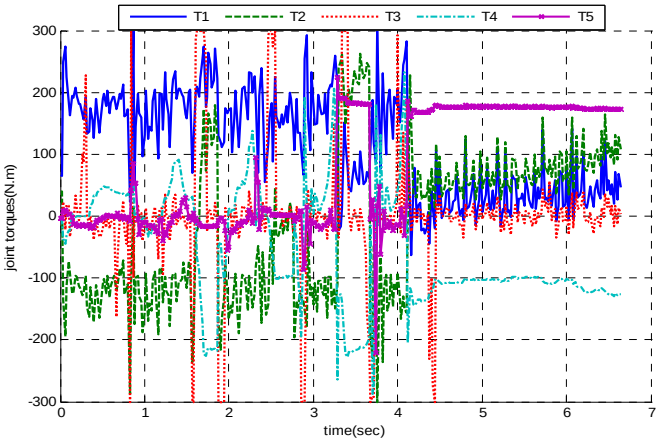

Fig. 11. Joint torques with measurement noise.

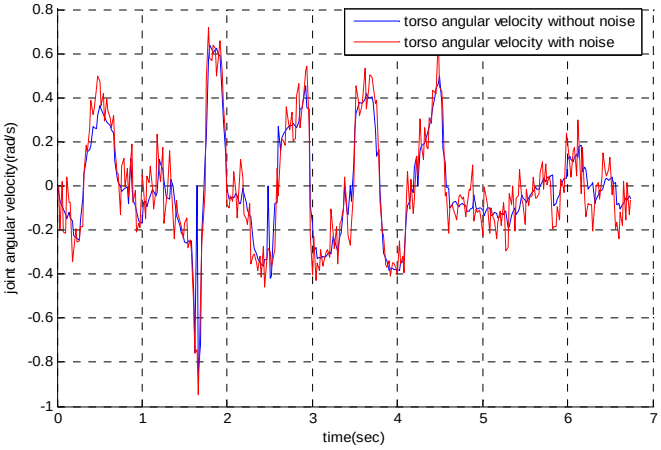

Fig. 9. Torso angular velocity with and without measurement noise.

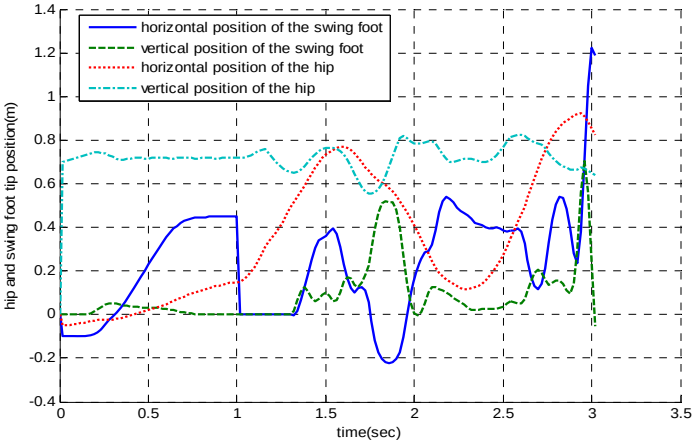

Fig. 12. Horizontal and vertical position of swing foot and hip without NDO.

REFERENCES

[1] Zohdy M. A. and Zaher A. A., "Robust control of biped' robots," *American Control Conference*, Chicaao, Illinois, 2000.

[2] Chuangfeng H. and Yuefa F., "Robust control for stable dynamic walking of biped robot," *International Conference on Intelligent Robots and Systems*, Beijing, China, 2006.

[3] Liu L. M., Tian Y. T, Sui1 Zh., and Huang X. L., "Finite-time robust trajectory tracking control for the under actuated biped robot based on poincarélike-alter-cell-to-cell mapping method," *4th International Conference on Autonomous Robots and Agents*, Wellington, pp. 686-691, New Zealand, 2009.

[4] Nakao M., Ohnishi K., and Miyachi, "A robust decentralized joint control based on interference estimation," *IEEE International Conference on Robotics and Automation*, Raleigh, NC, 1987.

[5] Smadi I. and Fujimoto Y., "On nonlinear disturbance observer base control of euler-lagrange systems," *Journal of System Design and Dynamics*, Vol. 3, No. 3, pp. 330-343, 2009.

[6] Gupta A., *Disturbance Observer Based Closed Loop Control of Haptic Interfaces*, PhD Dissertation, Department of Mechanical Engineering and Materials Science, Rice University, Houston, Texas, 2008.

[7] Young Doo Y., Jung E., and Sul S. k., "Application of a disturbance observer for a relative position control system," *IEEE Transactions on Industry Applications*, Vol. 46, Issue 2, 2010.

[8] Azevedo Ch., Poignet Ph., Espiau B., "Moving horizon control for biped robots without reference trajectory," *International Conference on Robotics & Automation*, Washington D.C., 2002.

[9] Azevedo CH., Poignet PH., and Espiau B., "Artificial locomotion control: from human to robots," *Journal of Robotics and Autonomous Systems*, Vol.43, pp. 203-223, 2004.

[10] Zhu Zh., Wang Y., and Chen X., "Real-time control of full actuated biped robot based on nonlinear model predictive control," *Intelligent Robotics and Applications*, Vol. 5314, pp. 873-882, Springer Verlag, 2008.

[11] Mu X., *Dynamics and Motion Regulation of a Five-link Biped Robot Walking in the Sagittal Plane*, PhD Thesis, Department of Mechanical and Manufacturing Engineering, University of Manitoba, Canada, 2004.

[12] Vukobratovic M. and Stepanenko Y., "Mathematical models of general anthropomorphic systems," *International Journal of Mathematical Biosciences*, Vol.17, pp.191-242. 1973.

[13] Mitobe K., Mori N., Nasu Y. and Adachi N. "Control of a biped walking robot during the double support phase," *Journal of Autonomous Robots,* Vol. 4, No. 3, pp. 287-296, 1997.

[14] Bagheri A., Felezi M., and Mousavi P. "Adaptive control and simulation of a seven-link biped robot for the combined trajectory motion and stability investigations," *WSEAS Transactions on Systems,* Vol. 5, No. 5, pp. 1214-1222, 2006.

[15] Diedam H., Dimitrov D., Wieber P., Mombaur K., and Diehl M., "Online walking gait generation with adaptive foot positioning through linear model predictive control," *International Conference on Intelligent Robots and Systems*, Nice, France, 2008.

[16] Dimitrov D., Wieber P., Ferreau H., and Diehl M., "On the implementation of model predictive control for on-line walking pattern generation," *International Conference on Robotics and Automation*, Pasadena, CA, USA, 2008.

[17] Wieber P., "Viability and predictive control for safe locomotion," *International Conference on Intelligent Robots and Systems*, Nice, France, 2008.

[18] A. Nikoobin and R. Haghighi, "Lyapunov-based nonlinear disturbance observer for serial n-link robot manipulators," *Journal of Intelligent and Robotic Systems*, Vol. 55, No. 2-3y, pp. 135-153, 2009.

[19] Espiau B. and Sardain P., "The anthropomorphic biped robot BIP2000," *IEEE International Conference on Robotics & Automation*, San Francisco, CA, 2000.

Biography oh Authors

Mohammad Farrokhi (M'92) has received his B.S. degree from K.N. Toosi University, Tehran, Iran, in 1985, and his M.S. and Ph.D. degrees from Syracuse University, Syracuse, New York, in 1989 and 1996, all in electrical engineering. In 1996, he joined Iran University of Science and Technology, where he is currently an Associate Professor of Electrical Engineering. His research interests include automatic control, fuzzy systems, and neural networks.

Mohsen Parsa was born in Isfahan, Iran, in 1985. He received his B.Sc. degree in Electrical Engineering from Islamic Azad University of Najaf Abad, Isfahan, Iran, in 2007, and M.Sc. degree from Iran University of Science and Technology, Tehran, Iran, in 2010. His research interests include model predictive control, intelligent control, disturbance observer and biped robots

.